Strong $L = 0$ (t, p) Transitions in the Even Isotopes of Ti, Cr, and Fe

R. F. Casten, E. R. Flynn, Ole Hansen, and T. J. Mulligan*
Los Alamos Scientific Laboratory, University of California,† Los Alamos, New Mexico 87544
(Received 5 February 1971)

Absolute differential cross sections for strong $L = 0$ (t,p) transitions on targets of ^{46,48,50}Ti, ^{50,52,54}Cr, and ^{54,56,58}Fe have been measured. The bombarding energy was 13 MeV and reaction angles of 12.5 and 20° were used. The data are compared with model predictions, with special emphasis on the pairing-vibrational model with isospin. The latter model correctly predicts the dependence on neutron number of the (t,p) cross sections but fails, as do all other models, to predict the steady cross-section decrease with increasing Z. It is suggested that the latter effect is caused by a slow change in the ground-state correlations.

I. INTRODUCTION

High-resolution (t, p) reaction data have been published for all the even isotopes of Ca, for ^{46,48}Ti, ^{50,52,54}Cr, and for ^{54,56}Fe.[1-4] The Ca experiment yielded cross sections in mb/sr but all the others gave differential cross sections in arbitrary nonrelated units. The primary aim of the present experiment was to obtain absolute cross sections for the (t, p) reactions on targets of the even isotopes of Ti, Cr, and Fe, with particular emphasis on the strong $0^+ \rightarrow 0^+$ transitions. Together with the Ca data this allows a test of the recent pairing-collective model with isospin included[5,6] over a rather wide range of nuclei. Models previously proposed for the even nuclei in this region have concentrated on the isotopes of a given element[7] or on the $f_{7/2}$ shell.[8] The pairing-collective model takes ^{56}Ni as the pairing ground state and predicts the 0^+ transition intensities in even nuclei from Ca to Se. The present experiment provides a test of these models through the $f_{7/2}$ shell and part of the f-p shell and, in addition, it provides an absolute cross-section scale for the transitions observed in the earlier work, relying only on a small distorted-wave correction to connect the present 13-MeV data with those at ≈12 MeV (Cr, Fe) and 11.14 MeV (^{48}Ti).

II. EXPERIMENTAL PROCEDURES

A. Targets

The targets were made by vacuum evaporation of a specially prepared sample of the metal of the relevant element. The samples, consisting of approximately equal amounts of the even isotopes of the element were prepared by the Isotopes Division of Oak Ridge National Laboratory from stock enrichments of the relevant isotopes. The final enrichments of each sample were determined by a mass-spectrometer analysis, the results of which are given in Table I. The targets were typically 40–60 μg/cm^2 thick and a carbon foil of similar thickness was used as a backing.

B. Procedures

The targets were bombarded with 13-MeV tritons from the Los Alamos tandem accelerator. First, the proton spectra from the three different elements were measured using an Elbek-type magnetic spectrograph and photographic plate detection. Data were taken at lab angles of 12.5 and 20° with respect to the beam; these angles were also used in the experiments quoted above.[1-4] (It was not possible in the present experimental arrangement to obtain a scattering angle of 5°.) In a second bombardment of each target a solid-state counter telescope was used as a detector; the telescope was linked to the SDS 930 on-line computer so that mass identification could be accurately performed.[9] In the counter experiments the (t, p) intensities were measured relative to the (t, t) intensities at 12.5 and 20°. The elastic scattering was measured from 12.5 to 30° in 2.5° intervals. In the case of Fe the counter-telescope experiment was made on a ^{58}Fe target (enriched) rather than on the ^{mix}Fe sample, whereas the Cr and Ti data were from the mixed isotope targets.

The absolute cross-section scales were established by normalizing the (t, t) data to optical-model calculations. The calculated elastic cross sections vary from about 80% of the Rutherford value at 12.5° to about 40% at 30°. This region is rather insensitive to variations in the optical potential, and the cross-section scales are believed to be accurate to within ±15%. Errors on the cross-section scales will constitute a systematic error for any given element, but do not affect the relative cross sections for the various isotopes of the element. The latter are probably accurate to ±10% for the ground-state transitions.

TABLE I. Isotopic composition of the targets in %. The numbers are from a mass-spectroscopic analysis made on the specific sample used for the relevant target and furnished by Oak Ridge National Laboratory.

Target element	Mass number 46	47	48	49	50	52	53	54	56	57	58
Ti	31.05 ±0.10	1.55 ±0.05	33.15 ±0.10	1.28 ±0.05	32.99 ±0.10						
Cr					26.88	38.12	0.98	34.02			
Fe								33.22 ±0.10	32.66 ±0.10	1.47 ±0.05	32.65 ±0.10

C. Results

A proton spectrum from the $^{mix}Cr(t, p)$ spectrograph experiment is shown in Fig. 1. The energy resolution was better than 15 keV full width at half maximum, and the strong $L = 0$ transitions indicated were readily identified by comparison with results from the literature. An independent check on the previous $L = 0$ assignments was obtained from the characteristic ratio $\sigma(12.5°)/\sigma(20°)$, and in all cases the present results agreed with the older assignments. The observed ground-state Q values, excitation energies, and 12.5° cross sections are shown in Table II in comparison with the results from Refs. 2–4. In the 11-MeV $^{48}Ti(t, p)$ experiment[2] as well as in the 12.15-MeV $^{50}Cr(t, p)$ experiment[3] two strong 0^+ transitions were observed. The relative intensities for the Cr transitions agree well with the present results, whereas there is some difference in the Ti case. Distorted-wave (DW) calculations indicate that some of the discrepancy in the Ti case stems from the different bombarding energies used in the two experiments.

III. ANALYSIS AND DISCUSSION

A. Distorted-Wave Procedures

The data were analyzed with the two-nucleon-transfer code TWOPAR by Bayman and Kallio[10] using the procedures of Flynn and Hansen.[11] One triton potential was taken from the work of Flynn, Armstrong, and Beery[12] (^{52}Cr), while a second potential had a somewhat lower absorption (see Table III) to take into account the high isospin of some of the target nuclei. Three different proton potentials were tried, all of Perey geometry,[13] but with different real and imaginary depths (see Table III). In terms of the Perey prescription [Eq. (2), Ref. 13] for the real well depth, the value V

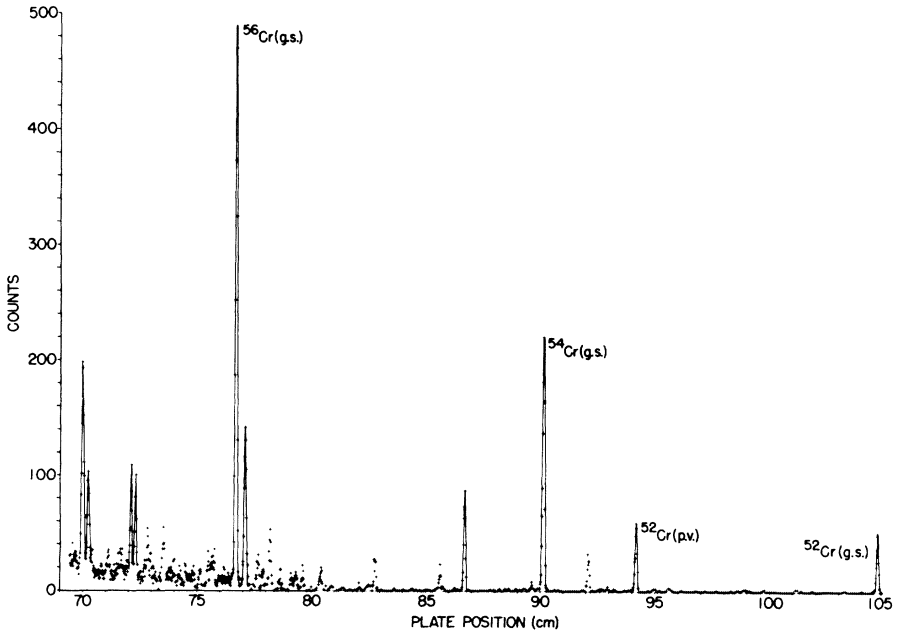

FIG. 1. Proton spectrum at 12.5° from the (t, p) reaction at 13.0 MeV on the mixed Cr target. The labeled peaks correspond to the strong 0^+ states in the Cr isotopes discussed in the text.

= 53 MeV corresponds to the lowest outgoing proton energy encountered in these experiments, whereas $V = 49$ MeV corresponds to the highest proton energy of interest.

Some comparisons between the $L = 0$ angular distributions predicted by TWOPAR and the ^{46}Ca and ^{48}Ca angular distributions from Ref. 1 are shown in Fig. 2. The combination of potentials FL2 and P1 (Table III) gives the best fits to these data. The Cr data show, though, a vague preference for the FL2, P2 combination. Combinations with P3 are ruled out by the data. The full analysis was made with the combinations FL2, P1 and FL2, P2. At forward angles the predicted cross sections for the first combination are from 6 to 18% larger than for the second combination. The combination FL1, P1 gives cross sections about 30% larger than from the FL2, P2 combination. The theoretical cross sections in the analysis given below are all from the FL2, P1 combination.

An absolute normalization of the DW cross sections is used in the discussions to follow. If the cross section calculated from the code is σ_{DW}, then[11]

$$(d\sigma/d\omega)_{DW} = 310 \times \sigma_{DW}(t, p) \text{ mb/sr} . \quad (1)$$

Here σ_{DW} contains the two-neutron spectroscopic amplitudes and the statistical factor $(2J_{final}+1)/(2J_{initial}+1)$, but it does not contain any isospin Clebsch-Gordan coefficients. The value of $N = 310$ corresponds to a value of D_0^2 of 25×10^4 MeV^2 fm^3 (see Flynn *et al.*[14]).

Absolute cross-section scales are provided for the previous (t, p) work by applying a DW calculat-

TABLE II. Strong $L = 0$ (t, p) transitions. The results from the present experiment are at 12.5° lab angle and $E_1 = 13.0$ MeV. Errors are discussed in the text: they are ±15% on the mb/sr scale for each element and ±10% for each number within the isotopes of an element.

Final nucleus	Q (keV) Present exp.	E_x (keV) Present exp.	Q (keV) Previous exp.	E_x (keV) Previous exp.	Relative scale arbitrary units Previous exp.	Relative scale arbitrary units Present exp.	mb/sr Present exp.	Ref.
^{48}Ti	12 021[a]	0	12 021[a]	0	100(5°)	100	1.10	
		4589 ± 15		4591 ± 15	25(5°)	20	0.22	b
		4967 ± 10		4974 ± 15	73(5°)	37	0.41	
^{50}Ti	10 591 ± 10	0	10 609[a]	0	100(5°)	100	0.96	
		3865 ± 10		3880 ± 15	170(5°)	129	1.24	c
				5633 ± 15	40(5°)			
^{52}Ti	5700 ± 10	0	5698 ± 10	0			2.38	d
^{52}Cr	12 823[a]	0	12 823[a]	0	100(5°)	100	0.57	
		2660 ± 10		2663 ± 15	117(5°)	100	0.57	e
		4745 ± 10		4749 ± 15	27(5°)	28	0.16	
^{54}Cr	9171 ± 10	0	9181[a]	0			1.44	f
^{56}Cr	6024 ± 10	0	5995 ± 30	0			3.13	g
^{56}Fe	12 021[a]	0	12 021[a]	0			1.12	h
^{58}Fe	9209 ± 15	0	9202[a]	0			1.70	i
^{60}Fe	6907 ± 15	0	7025[a]	0			2.51	j

[a] Mass Q values from J. Mattauch, W. Thiele, and A. Wapstra, Nucl. Phys. 67, 32 (1965).

[b] The experiment of Ref. 2 was performed at $E_1 = 9.64$ MeV; the cross sections for ^{46}Ti$(t,p)^{48}$Ti from Ref. 2 should not be compared directly with the present data.

[c] See Ref. 2. $E_1 = 11.14$ MeV.

[d] See D. C. Williams, J. D. Knight, and W. T. Leland, Phys. Letters 22, 162 (1966). $E_1 = 7.5$ MeV. No excited 0^+ states reported.

[e] See Ref. 3. $E_1 = 12.15$ MeV.

[f] See Ref. 3. $E_1 = 11.95$ MeV. Excited 0^+ states were found at 4009 and at 4572 keV with intensities of 6 and 19% of the ground-state transition, respectively.

[g] See Ref. 3. $E_1 = 11.99$ MeV. An excited 0^+ state at 3.897 MeV was excited with 4% of the ground-state cross section.

[h] See Ref. 4. $E_1 = 12$ MeV. Several excited $L = 0$ transitions were observed, the strongest leading to a state at 3.60 MeV with 14% of the ground-state cross section.

[i] See Ref. 4. $E_1 = 12$ MeV. The strongest $L = 0$ transition above the ground state is to the 2.26-MeV level, and it proceeds with 10% of the ground-state cross section.

[j] Not reported before.

TABLE III. Optical-model potentials. The optical potentials were of the Woods-Saxon shape. The notation is standard.

Particle	Label	V	W (MeV)	W_D'	r_0	a	r_0' (fm)	a'	r_{0c}	λ
t	FL1	165.4	12	0	1.16	0.75	1.50	0.75	1.3	
	FL2	165.4	16.4	0	1.16	0.75	1.50	0.75	1.3	
p	P1	53	0	15.5	1.25	0.65	1.25	0.47	1.25	
	P2	49	0	15.5	1.25	0.65	1.25	0.47	1.25	
	P3	49	0	12.5	1.25	0.65	1.25	0.47	1.25	
n-n	BS	a	0	0	1.27	0.65				25

[a]Adjusted to give a binding to each particle of 0.5 $[Q(t,p)+8.482]$ MeV. The triton rms radius was taken to be 1.7 fm.

ed correction to our absolute cross sections at 13 MeV and 12.5° to convert them to the conditions of Refs. 2–4. The correction factor varies slowly with energy, mass, Q value, and configuration; hence, within the accuracy expected, one such factor is sufficient for the Cr and Fe data at ~12 MeV and 5° and one for the ^{48}Ti data at 11.14 MeV and 5°. For the Cr, Fe data our 0^+ cross sections must be multiplied by 2.72, while for ^{48}Ti they must be multiplied by 2.85 to yield effective cross sections applying to the experimental conditions of Refs. 2–4. For example, the ^{52}Cr$(t, p)^{54}$Cr ground-state cross section of 1.44 mb/sr found here implied a 12 MeV, 5° cross section of 3.9 mb/sr which corresponds to the number 890 quoted in Ref. 3, Table 3. These correction factors should be accurate to ±30%, and result mainly from the change in angle rather than in bombarding energy.

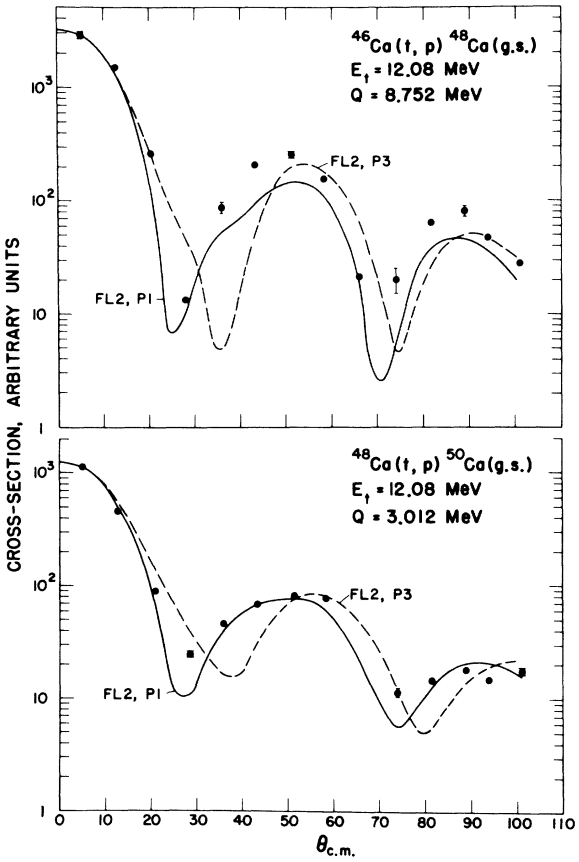

FIG. 2. Comparison of measured and calculated $L = 0$ (t,p) angular distributions in the Ca isotopes. The data are taken from Ref. 1. The calculated distributions were obtained using the code TWOPAR and the optical potentials indicated (see Table III).

B. Pairing-Vibrational Model with Isospin

A pairing-vibrational description of the 0^+ states around $N = 28$ has been proposed by Bohr,[5] Nathan[15] and recently in more detail by Bayman, Bes, and Broglia.[6]

The ground state of doubly magic ^{56}Ni (with isospin $T = 0$) is taken as the reference, vacuum state $|0\rangle$. The operator $\Gamma^\dagger(\alpha = 2)$ which creates the ground state of ^{58}Ni,

$$|^{58}\mathrm{Ni}(0)\rangle = \Gamma^\dagger(\alpha = 2, T = T_z = 1)\,|0\rangle, \tag{2}$$

and the operator $\Gamma^\dagger(\alpha = -2)$ that leads from ^{56}Ni(0) to ^{54}Ni(0),

$$|^{54}\mathrm{Ni}(0)\rangle = \Gamma^\dagger(\alpha = -2, T = 1, T_z = -1)\,|0\rangle, \tag{3}$$

are the fundamental excitations of the scheme. The pair-creation operator $\Gamma^\dagger(\alpha = 2, T = T_z = 1)$ adds a pair of neutrons with intrinsic spin $S = 0$ which are scattered primarily over $2p_{3/2}$, $2p_{1/2}$, and $1f_{5/2}$ orbits in some definite way. Since the scheme introduces ground-state correlations in the vacuum state $|0\rangle$ of two-particle–two-hole, four-particle–four-hole, etc. character, the $\Gamma^\dagger(\alpha = 2)$ operator also to some extent adds pairs of particles in the shell below, $1f_{7/2}$, $2s_{1/2}$, and $1d_{3/2}$. Conversely, the pair-removal operator $\Gamma^\dagger(\alpha = -2)$ predominantly destroys a correlated pair of nucleons in the $1f_{7/2}$, $2s_{1/2}$, and $1d_{3/2}$ orbits and to a lesser extent it destroys pairs in the $2p_{3/2}$, $2p_{1/2}$, $1f_{5/2}$ orbits. It is specifically assumed that the structure of the $\Gamma^\dagger$ operators does not depend on T_z. Hence the scheme handles proton-proton and proton-neutron $(T = 1, S = 0)$ correlations on the

same footing as the neutron-neutron correlations.

The excited states in the scheme are built by suitable stacking of the two fundamental excitations (harmonic approximation), which excitations are treated as bosons. Hence $(\Gamma^{\dagger})^n$ can yield $T = 0, 2, 4, \ldots n$ if n is even, and $T = 1, 3, 5, \ldots n$ if n is odd. The isospin coupling scheme is defined by combining the isospins of the n_r removal operators $[\Gamma^{\dagger}(\alpha = -2)]$ to T_r, then the isospin of the n_a addition operators $[\Gamma^{\dagger}(\alpha = 2)]$ to T_a, and finally by coupling T_r with T_a to give the total isospin of the state T and its z component T_z. Hence any state in the scheme is characterized by the quantum numbers

$$(n_r T_r, n_a T_a, T T_z) . \tag{4}$$

The assignments given to the various levels involved in the present analysis are shown in Table IV.

The energy relations implied by the vibrational scheme will not be dealt with here, since the observed energies can be accounted for equally well by the vibrational and the rotational schemes, and hence the energies do not distinguish which of the schemes is in better agreement with experiment (see Ref. 6).

The intensity relations for two-nucleon-transfer reactions were derived in Ref. 6, and they may be written

$$\sigma_a = \alpha_a \langle T T_z 1 (T_z' - T_z) | T' T_z' \rangle^2 \langle 1 (t_z' - t_z) \tfrac{1}{2} t_z | \tfrac{1}{2} t_z' \rangle^2 (2T_a' + 1)(2T + 1)$$
$$\times \begin{Bmatrix} T_r & T' & T_a' \\ 1 & T_a & T \end{Bmatrix}^2 \left[\delta(T_a', T_a + 1) \frac{(T_a + 1)(n_a + T_a + 3)}{(2T_a + 3)} + \delta(T_a', T_a - 1) \frac{T_a (n_a - T_a + 2)}{(2T_a - 1)} \right] \tag{5}$$

for a transition

$$(\tfrac{1}{2}, t_z) + (n_r T_r, n_a T_a, T T_z) - (\tfrac{1}{2} t_z') + (n_r T_r, n_a + 1 T_a', T' T_z') ,$$

and

$$\sigma_r = \alpha_r \langle T' T_z' 1 (T_z - T_z') | T T_z \rangle^2 \langle 1 (t_z' - t_z) \tfrac{1}{2} t_z | \tfrac{1}{2} t_z' \rangle^2 (2T_r' + 1)(2T' + 1)$$
$$\times \begin{Bmatrix} T_a & T' & T_r' \\ 1 & T_r & T \end{Bmatrix}^2 \left[\delta(T_r', T_r + 1) \frac{(T_r + 1)(n_r + T_r + 3)}{(2T_r + 3)} + \delta(T_r', T_r - 1) \frac{T_r (n_r - T_r + 2)}{2T_r - 1} \right] \tag{6}$$

for a transition

$$(\tfrac{1}{2}, t_z) + (n_r T_r, n_a T_a, T T_z) - (\tfrac{1}{2}, t_z') + (n_r + 1\, T_r', n_a T_a, T' T_z') .$$

Here the lower case t's designate isospins of the incoming and outgoing light particles. The first equation is useful for a (t, p) transition if the two neutrons are predominantly deposited in the $p_{3/2}$, $p_{1/2}$, $f_{5/2}$ shell, whereas Eq. (6) corresponds to pickup of two nucleons mainly from the s, d, and f orbits and applies to the (p, t) reaction. Equations (5) and (6), however, are valid for the inverse processes as well. For the (t, p) reactions the product of the isospin Clebsch-Gordan coefficients is always $\frac{2}{3}$.

Two simple features emerge from Eqs. (5) and (6).
(i) If T_a and T_a' have their maximum values in Eq. (5), i.e., they equal n_a and $n_a + 1$, respectively, then

$$\sigma_a \propto (n_a + 1) . \tag{7}$$

The cross section for pair addition varies like 1:2:3, etc., as neutron pairs are placed into the $p_{3/2}$, $p_{1/2}$, $f_{5/2}$ orbits. This result, modified by a small Q-dependent correction, will be evident below for the Fe and the heavier Cr isotopes.
(ii) Transitions with the same T and T' [Eq. (6)] will have

$$\sigma_r \propto (n_r + 1) . \tag{8}$$

The comparison between theory and experiment was made using the semiempirical Ca form factors of Ref. 11. The ^{46}Ca – ^{48}Ca(g.s.) form factor was used for all transitions obeying Eq. (6), while the ^{48}Ca – ^{50}Ca(g.s.) form factor was employed for all Eq. (5) transitions. Using the normalization specified by Eq. (1) these form factors predict the ^{46}Ca – ^{48}Ca(g.s.) and ^{48}Ca – ^{50}Ca(g.s.) cross sections as 1.45 and 3.21 mb/sr, respectively, in very good agreement with the experimental numbers 1.48 and 3.24 mb/sr, respectively. Thus, with the form factors used, the absolute cross-section scale as well as the relative increase in cross section caused by the $N = 28$ shell closure are correctly predicted.

The present DW analysis differs from that quoted in Ref. 11 because of a small error discovered in the DW code[16] subsequent to the publication of Ref. 11. The error also affects the other (t, p) cross sections used in Ref. 11 but to a smaller extent. The result $N = 310$ is changed by <6% and we

have therefore continued to use the published number.

Predictions $\sigma_{DW}(Z, N, E, Q)$ were calculated for all the transitions of Table IV using the appropriate bombarding energies and Q values. The theoretical cross sections given in Table IV are $\sigma_{DW}(Z, N, E, Q)$ multiplied by $\sigma_{r,a}(Z, N)/\sigma_{r,a}(^{48}\mathrm{Ca})$, where the $\sigma_{r,a}$ were calculated from either Eq. (5) (σ_a) or from Eq. (6) (σ_r). $\sigma_r(^{48}\mathrm{Ca})$ is $\sigma_r(^{46}\mathrm{Ca} \rightarrow {}^{48}\mathrm{Ca}(\mathrm{g.s.}))$ and $\sigma_a(^{48}\mathrm{Ca})$ stands for $\sigma_a(^{48}\mathrm{Ca} \rightarrow {}^{50}\mathrm{Ca}(\mathrm{g.s.}))$. Table V lists the ratios of experimental to theoretical ground-state cross sections displayed as a function of N and Z. In the region just around ^{48}Ca there is quite good agreement between experiment and theory, but as one moves away from this nucleus discrepancies on the order of a factor of 4 to 10 develop.

The cross sections of the $N = 26 \rightarrow 28$ and the $N = 28 \rightarrow 30$ ground-state transitions fall off rather strongly as a function of Z, a trend that is only vaguely apparent in the model predictions (see Table IV). This smooth falloff is apparently not accompanied by a fractionation, whereas the transitions to excited 0^+ states usually are fractionated.[1-4] The total strength to excited 0^+ states other than those quoted in Table IV may be as much as 50% of the cross section for the transition cited in the table [e.g., $^{44}\mathrm{Ca} \rightarrow {}^{46}\mathrm{Ca}$ (Ref. 1) and $^{50}\mathrm{Cr} \rightarrow {}^{52}\mathrm{Cr}$ (Ref. 3)].

The N dependence of the ground-state (t, p) cross sections is in quite good agreement with the model predictions (see Tables IV and V), although for $N \leq 24$ the predicted cross sections increase with decreasing N somewhat faster than the experimental intensities. The ratio $\sigma(N = 26 \rightarrow 28)/\sigma(N = 28 \rightarrow 30)$ is about constant, as predicted by the model. The $\sigma(N = 28 \rightarrow 30) : \sigma(N = 30 \rightarrow 32) : \sigma(N = 32 \rightarrow 34)$ is predicted as $\approx 1 : 2$ for Cr and as $\approx 1 : 2.0 : 2.8$ for Fe. The experimental numbers are 1:2.2 and 1: 1.5: 2.2, respectively. [Note that the theoretical σ values incorporate Q value effects and hence differ from the rule of Eq. (7).]

In summary, the pairing-vibrational model correctly predicts the N dependence of the (t, p) ground-state cross sections. It predicts excited 0^+ states for $N_{\mathrm{target}} \leq 26$ and no excited 0^+ strength for $N_{\mathrm{target}} \geq 28$, in agreement with experiment. However, for $N_{\mathrm{target}} \leq 26$ it considerably overestimates the observed excited 0^+-state cross sections. It fails to predict the observed Z dependence of the cross sections.

C. Pairing Rotational Model with Isospin

This model[6] is based on the superconducting extreme of the pairing model, and hence the $N = 28$ shell closure in this picture is completely washed out. The model predicts an excited 0^+ state with

TABLE IV. Pairing-vibrational analysis.

Target nucleus	Final nucleus	E_x (MeV)	Quantum numbers $(n_r T_r; n_a T_a; T T_z)$ Target	Final	σ_{exp} [a]	σ_{theory}	$\frac{\sigma_{\mathrm{exp}}}{\sigma_{\mathrm{theory}}}$	Comments
^{42}Ca	^{44}Ca	0	71; 00; 11	62; 00; 22	2.4	4.3	0.56	
^{44}Ca	^{46}Ca	0	62; 00; 22	53; 00; 33	2.0	2.9	0.69	
^{46}Ca	^{48}Ca	0	53; 00; 33	44; 00; 44	1.5	1.5	1.0	$N = 26 \rightarrow 28$
^{48}Ca	^{50}Ca	0	44; 00; 44	44; 11; 55	3.2	3.2	1.0	$N = 28 \rightarrow 30$
^{46}Ti	^{48}Ti	0	51; 00; 11	42; 00; 22	1.1	2.2	0.50	
^{48}Ti	^{50}Ti	0	42; 00; 22	33; 00; 33	1.0	1.1	0.90	$N = 26 \rightarrow 28$
^{50}Ti	^{52}Ti	0	33; 00; 33	33; 11; 44	2.4	2.9	0.83	$N = 28 \rightarrow 30$
^{50}Cr	^{52}Cr	0	31; 00; 11	22; 00; 22	0.57	0.91	0.63	$N = 26 \rightarrow 28$
^{52}Cr	^{54}Cr	0	22; 00; 22	22; 11; 33	1.4	2.5	0.56	$N = 28 \rightarrow 30$
^{54}Cr	^{56}Cr	0	22; 11; 33	22; 22; 44	3.1	5.0	0.62	
^{54}Fe	^{56}Fe	0	11; 00; 11	11; 11; 22	1.1	2.2	0.50	$N = 28 \rightarrow 30$
^{56}Fe	^{58}Fe	0	11; 11; 22	11; 22; 33	1.7	4.4	0.39	
^{58}Fe	^{60}Fe	0	11; 22; 33	11; 33; 44	2.5	6.2	0.40	
^{42}Ca	^{44}Ca	5.86	71; 00; 11	71; 11; 22	1.5	4.3	0.35	
^{44}Ca	^{46}Ca	5.60	62; 00; 22	62; 11; 33	1.9	4.0	0.48	
^{46}Ca	^{48}Ca	5.46	53; 00; 33	53; 11; 44	3.0	3.6	0.83	
^{46}Ti	^{48}Ti	4.97	51; 00; 11	51; 11; 22	0.4	3.5	0.11	
^{48}Ti	^{50}Ti	3.88	42; 00; 22	42; 11; 33	1.2	3.3	0.36	
^{50}Cr	^{52}Cr	2.66	31; 00; 11	31; 11; 22	0.57	2.6	0.22	

[a] The Ca data are taken from Ref. 1; all other data are from the present experiment. The cross sections are in mb/sr.

TABLE V. N and Z dependence of ratios of experimental and pairing-vibrational (t,p) cross sections for ground states.

Element	Final-state neutron number 24	26	28	30	32	34
Ca	0.56	0.69	1.0	1.0		
Ti		0.50	0.90	0.83		
Cr			0.63	0.56	0.62	
Fe				0.50	0.39	0.40

TABLE VI. N and Z dependence of ratios of experimental and MBZ-model (t,p) cross sections for ground states.

Element	Final-state neutron number 22	24	26	28
Ca	1.0	1.0	0.9	1.0
Ti			1.5	1.0
Cr				0.8

a cross section similar to the ground-state intensity for $N_{\text{final}} \leq 28$ as well as for $N_{\text{final}} > 28$. Thus this model fails with regard to Z dependence, N dependence, and excited 0^+ strength.

D. Microscopic Approach

Microscopic calculations with a pairing Hamiltonian and a configuration space consisting of the $2s_{1/2}$, $1d_{3/2}$, $1f_{7/2}$, $2p_{3/2}$, $2p_{1/2}$, and $1f_{5/2}$ orbitals have been published by Bayman and Hintz for the Ca case.[17] They found quite reasonable agreement with experiment. Recently an extensive shell-model calculation for Ca has been published by Federman and Pittel[7]; they find good qualitative agreement with the (t, p) data although no DW calculations were made. Outside of Ca no adequate microscopic calculations are available. The $f_{7/2}$ model wave functions of McCullen, Bayman, and Zamick[8] give absolute cross sections that are about a factor of 6 too small. However, the relative ground-state cross sections within the Ca isotopes agree well with the experimental trend as has been pointed out previously.[17] For the three Ti and Cr transitions occurring within the $f_{7/2}$ shell the agreement for relative cross sections is also reasonable (see Table VI) and at least as acceptable as that of the pairing-vibrational model.

E. Summary and Discussion

The fact that the $N = 26 \rightarrow 28$ and the $N = 28 \rightarrow 30$ ground-state cross sections decrease with increasing Z without any observable fractionation suggests that the cause for this behavior is a change in the ground-state correlations. The importance of such correlations is demonstrated by the DW calculations of the ^{46}Ca$(t, p)^{48}$Ca(g.s.) cross section. Using an N of 310, a $d\sigma/d\omega$ at 5° of 0.5 mb/sr is calculated with a pure $(f_{7/2})^2$ form factor. Using instead a form factor $0.97(1f_{7/2})^2 - 0.14(2s_{1/2})^2 - 0.19(1d_{3/2})^2$ incorporating s-d shell correlations, a cross section three times larger is predicted (1.5 mb/sr). Finally allowing p mixtures too, $0.94(f_{7/2})^2 - 0.14(2s_{1/2})^2 - 0.19(1d_{3/2})^2 + 0.22(p_{3/2})^2 + 0.097(p_{1/2})^2$, a cross section of 3.0 mb/sr is calculated, i.e., six times the $(f_{7/2})^2$ value. (The last form factor is from Ref. 11 and is the one used in Table IV.) Hence the (t, p) reaction in this region is very sensitive to small admixtures of s and d holes, and it appears that the extent of these admixtures largely determines the cross-section magnitude. Therefore, small changes in the admixture will greatly influence the cross sections, and it seems reasonable to connect the observed Z dependence with a gradual filling of the s and d neutron holes and an increase in p mixing as the single-particle levels are shifted as a function of proton number. (See also the arguments in works of Cohen[18] and Yagi.[19])

The excellent assistance of the Van de Graaff staff at Los Alamos is greatly acknowledged as is the help given us by Stuart Orbesen in taking the data. We are grateful to B. F. Bayman, D. R. Bes, and R. A. Broglia for many instructive discussions.

---

*An Associated Western Universities Fellow from Florida State University.

†Work supported under the auspices of the U. S. Atomic Energy Commission.

[1]J. H. Bjerregaard, O. Hansen, O. Nathan, R. Chapman, S. Hinds, and R. Middleton, Nucl. Phys. A103, 33 (1967).

[2]S. Hinds and R. Middleton, Nucl. Phys. A92, 422 (1967).

[3]R. Chapman, S. Hinds, and A. E. MacGregor, Nucl. Phys. A119, 305 (1968).

[4]B. L. Cohen and R. Middleton, Phys. Rev. 146, 748 (1966); B. L. Cohen, C. L. Fink, J. B. Moorhead, and R. A. Moyer, *ibid.* 157, 1033 (1967).

[5]A. Bohr, *Nuclear Structure* (International Atomic Energy Agency, Vienna, Austria, 1968), p. 179.

[6]B. F. Bayman, D. R. Bes, and R. A. Broglia, Phys. Rev. Letters 23, 1299 (1969).

[7]P. Federman and S. Pittel, Nucl. Phys. A155, 161 (1970).

[8]J. D. McCullen, B. F. Bayman, and L. Zamick, Phys. Rev. 134, B515 (1964).

[9]D. D. Armstrong, J. G. Beery, E. R. Flynn, W. S.

Hall, P. W. Keaton, Jr., and M. P. Kellogg, Nucl. Instr. Methods 70, 69 (1969).
[10]B. F. Bayman and A. Kallio, Phys. Rev. 156, 1121 (1967).
[11]E. R. Flynn and O. Hansen, Phys. Letters 31B, 135 (1970).
[12]E. R. Flynn, D. D. Armstrong, J. G. Beery, and A. G. Blair, Phys. Rev. 182, 1113 (1969).
[13]F. G. Perey, Phys. Rev. 131, 745 (1965).
[14]E. R. Flynn, R. F. Casten, O. Hansen, and T. J. Mulligan, to be published.
[15]O. Nathan, *Nuclear Structure* (International Atomic Energy Agency, Vienna, Austria, 1969), p. 191.
[16]B. F. Bayman, private communication.
[17]B. F. Bayman and N. M. Hintz, Phys. Rev. 172, 1113 (1968).
[18]B. L. Cohen, Phys. Letters 27B, 271 (1968).
[19]K. Yagi, Phys. Letters 28B, 455 (1969).

PHYSICAL REVIEW C VOLUME 4, NUMBER 1 JULY 1971

Differential Recoil Study of the $^{25}Mg(p, 2p)^{24}Na$ Reaction*

F. Michael Kiely†‡ and Albert A. Caretto, Jr.
Department of Chemistry, Carnegie-Mellon University, Pittsburgh, Pennsylvania 15213

(Received 12 June 1970)

Differential recoil spectra for the $^{25}Mg(p, 2p)^{24}Na$ reaction have been measured radiochemically at recoil angles of 90 and 60° for an incident energy of 300 MeV and at a recoil angle of 90° for 100-MeV bombarding energy. All the spectra display two peaks. The position of the lower-energy peak seems to remain unchanged with a shift in incident energy, while the higher-energy peak shifts to higher kinetic energies with an increase in bombarding energy. The results are compared with the spectra calculated from a plane-wave impulse-approximation calculation which assumes that only the $1d_{5/2}$ protons in ^{25}Mg are available for interaction. Limited agreement is obtained.

INTRODUCTION

In recent years, considerable interest has been shown in the mechanism of high-energy proton-induced nuclear reactions. In particular, the mechanism of the so-called "simple" reactions has been under investigation for some time.[1] For the most part, experimental investigations of these reactions have consisted of the measurement of production rates for the various reactions, as well as the determination of the change in these rates, as the incident proton energy is varied.[1,2]

More recently, several experiments have been performed in which the integral recoil properties of a few of these reactions have been measured.[3-5] In these experiments, the amount of product activity recoiling out of the target into the forward, backward, and perpendicular hemispheres is measured relative to the activity remaining in the target foil itself. Such studies suffer from two major disadvantages: (a) Because of collection of the total activity in a particular direction, only the average recoil kinetic energy can be inferred and consequently any possible structure in the recoil energy spectrum is lost; and (b) since the activity is collected in a 2π geometry, the nature of the angular distribution of the recoils and its effects on the derived average recoil kinetic energy is unknown.

Several workers[6,7] have measured the differential recoil spectrum for the product of a "simple" reaction. In these experiments, the distribution of product nuclei as a function of recoil kinetic energy is measured directly, thereby eliminating one of the difficulties of the integral recoil measurements. Other investigators have measured integral angular distributions of such reactions both separately[8] and as companion studies to the recoil measurements.[6,7] However, such treatments suffer from the difficulties encountered in trying to unfold the effects of the angular distribution and the energy spectrum on each other. Ideally, it is desirable to measure the energy spectrum as a function of the recoil angle in order to eliminate the geometrical averaging which confuses the interpretation given to the recoil spectrum.

Theoretical investigations of the "simple" reactions have for the most part been based on the Serber model and have employed Monte Carlo techniques in the numerical calculations.[9,10] It has been suggested[1,11] that "simple" reactions may be more properly described by a treatment giving more consideration to the quantum mechanical structure of the nucleus than does the Serber model. Benioff and Person[11] have recently performed such calculations, and their agreement with the small amount of available data is encouraging.

The purposes of the present work are: (a) to measure the differential recoil spectrum of a